

# Impact of Radial Heterogeneities of Biological Tissues on Dielectric Measurements

A. La Gioia<sup>1</sup>

E. Porter<sup>1</sup>

S. Salahuddin<sup>1</sup>

M. O'Halloran<sup>1</sup>

**Abstract** – The dielectric properties of biological tissues are relevant in dosimetry studies and in radio-frequency and microwave medical applications. Broadband tissue dielectric data is commonly acquired using open-ended coaxial probe techniques. In the last decades, several dielectric studies were conducted with the aim of increasing accuracy and repeatability of open-ended coaxial probe measurements. However, among recent studies, there are still inconsistencies in the procedure of dielectric characterisation of heterogeneous tissues. These inconsistencies arise from the fact that the open-ended coaxial probe design is based on the assumption that the investigated material is homogeneous. In order to accurately characterise heterogeneous tissues, it is necessary to conduct a meticulous histological analysis of the tissue types involved in the dielectric measurement. To this extent, it is fundamental to evaluate the tissue volume interrogated by the probe, also known as the probe sensing volume or histology region. In this study, early-stage experiments are presented to investigate how radial heterogeneities can impact the histology depth. The findings of this study confirm that the histology depth depends on the dielectric properties of the constituent tissue types and, then, demonstrate that radial heterogeneities have a significant impact on the evaluation of the probe histology depth. This work aims to provide the basis for more accurate dielectric characterisation of heterogeneous tissues to support microwave medical device design.

## 1 INTRODUCTION

The dielectric properties of biological tissues determine how each tissue transmits, absorbs, and reflects electromagnetic (EM) radiation. These properties are defined by relative permittivity,  $\epsilon_r$  (or  $\epsilon'$ ), and conductivity,  $\sigma$ , which are frequency- and temperature-dependent. Accurate dielectric characterisation of biological tissues represents the basis for the design and development of EM-based novel medical applications. In particular, accurate knowledge of the dielectric contrast between malignant and benign tissues in the microwave (MW) range is vital to the development and optimisation of novel MW imaging systems, and therapeutic procedures, such as hyperthermia and MW ablation.

The dielectric properties of biological tissues are commonly measured by the open-ended coaxial probe technique [1], [2]. Although dielectric data acquisition with this technique appears straightforward, different practices in the tissue measurement procedure may result in different experimental outcomes. In the past, a number of factors that introduce errors and uncertainties in the tissue measurement procedure were analysed, and best-practices were developed to compensate for equipment and sample preparation related errors [3]. However, standard procedures for the dielectric characterisation of highly heterogeneous tissues, such as cancerous and inflamed tissues, have not been developed.

Since the coaxial probe technique is based on the assumption that the investigated material is homogeneous, there is no clear procedure to dealing with the dielectric measurements of highly heterogeneous tissues. In order to minimise the data uncertainty related to the tissue complexity, it is necessary to conduct a meticulous histological analysis of the tissue types involved in the dielectric measurement [2], [4]. In the literature, there is no consistency in the evaluation of the tissue volume interrogated by the probe, also known as the probe sensing volume or histology region (since the probe sensing volume defines the tissue region that undergoes histological analysis). Thus it is unclear how best to select the portion of the sample to analyse histologically.

The histology region is delineated by the histology depth and radius, which circumscribe the volume of tissues that contribute to the dielectric properties measured by the probe. Because the histology region is related to the tissue composition of the measured sample, previous studies have examined the effect of different material combinations on the histology region. While, in these studies, the histology region has been investigated by analysing the histology depth and radius separately [5]–[7], in this work, we analyse how radial heterogeneities can impact the histology depth. Specifically, we prepare tissue phantoms with added radial heterogeneities, measure their dielectric properties and then calculate the histology depth of the different heterogeneous materials based on the definition given in [8]. In particular, the histology depth is calculated from two layered phantom samples, composed of a material of variable thickness in contact with the probe and a material of fixed thickness interfacing the material in contact with the probe. For simplicity, the material in contact with the probe (first layer material) is liquid, while the other material (second layer material) is solid. Thus, the distance from the material interface is gradually increased, starting from zero (at which distance only the second layer material is measured). Then, the histology depth is defined as the distance at which the second layer material ceases to contribute to the measured dielectric properties, within the uncertainty of the measurement (i.e., the distance at which only the permittivity of the first layer material is detectable, within the uncertainty of the measurement). Schematised information about the estimation of the histology depth is included in [8].

The paper is organised as follows. In the next section, the dielectric measurement set-up is

<sup>1</sup> Department of Electrical and Electronic Engineering, National University of Ireland, Galway, Ireland, email: [a.lagioia@nuigalway.ie](mailto:a.lagioia@nuigalway.ie), tel: +353 838478220

introduced, the measurement uncertainty of the system is calculated, and the phantom sample combinations are described. In Section 3, experimental results are reported and discussed. Lastly, in Section 4, the experimental outcomes are summarised.

## 2 MEASUREMENT METHODOLOGY AND MATERIALS

In this section, we describe the measurement calibration and validation (subsection 2.1), and report the experimental design used to evaluate the impact of radial heterogeneities on the histology depth (subsection 2.2).

### 2.1 Measurement calibration and validation

In this study, dielectric properties were measured using the Keysight slim form probe [9] connected to the Agilent E8362B network analyser. The Keysight slim form probe is the most commonly used probe in recent works, due to its small diameter (2.2 mm) [4], [10]. The probe was calibrated using the three-load standard procedure. After each calibration, the quality of the calibration was verified by measuring the dielectric properties of the 0.1 M NaCl solution, one of the most commonly used reference liquids [3], [11]. The measured dielectric signal was compared to the model described in [11]. In this way, the measurement accuracy, defined as the average percentage difference between the dielectric properties of the acquired data and the model, was calculated. If the measurement accuracy was within 3%, the calibration was determined to be of high quality and sample measurements were performed; otherwise the calibration procedure was repeated. The reference liquid accuracy was also taken into account in determining the uncertainty of any following sample measurements. Each liquid/solid sample was brought towards the probe by a lift table to minimise system perturbation. At each dielectric measurement, relative permittivity and conductivity were acquired at 101 frequency points over the microwave frequency range of 500 MHz – 20 GHz and the sample temperature was recorded.

### 2.2 Experimental design

Tissue-mimicking phantoms were fabricated to evaluate how the histology depth depends, not only on the dielectric properties of the materials distributed along the longitudinal extent of the histology region, but also on the properties of the materials distributed along the radial extent of the histology region. In particular, we manufactured samples using: 0.1 M NaCl (saline), air, and rubber-based tissue-mimicking phantoms. The tissue-mimicking phantoms are based on those developed in [12], and have a stable, solid structure. Two types of rubber-based phantoms were

used: one has low permittivity and the other one has high permittivity. In this paper, we denote the low permittivity phantom as ‘Phantom A’ and the high permittivity phantom as ‘Phantom B’.

From the materials listed above, two controlled heterogeneous samples were fabricated. The two samples are composed of two layers: the first layer material, which is in contact with the probe, is saline for one sample and air for the other one; the second layer material, which is separated from the probe by the first layer material, is the same for both samples and consists of Phantom A and Phantom B placed side by side. The top and the front views of the heterogeneous samples are schematised in Fig.1. From the front view image, it is clear that saline and air constitute the first layer material of the two samples and the second layer material is composed of Phantom A and Phantom B, for both samples. However, the second layer material is different at each of the three measurement locations: Phantom A at one point, Phantom B at the second point, and approximately 50% Phantom A and 50% Phantom B at the other point. Per each sample, the histology depths from the three measurement locations are calculated by varying the probe-material interface distance (corresponding to the thickness of the first layer material). Specifically, the probe-material interface distance was gradually increased by bringing down the lift table. The lift table was moved down, from the probe-material interface distance of 0 mm, at 0.1 mm steps (controlled by a micrometer) for a total distance of 1.5 mm that is equivalent to the maximum thickness of the first layer material. Per each sample, this set of experiments was repeated fully after each of three calibrations.

In particular, in the experimental design of this study, air and saline were selected because of the high contrast in permittivity, since the histology depth is strongly affected by the first layer material permittivity. Also, the two rubber-based phantoms have high contrast in permittivity to easily interpret the experimental results discussed in the following section.

## 3 RESULTS AND DISCUSSION

Before calculating the histology depth at the three measurement locations of the two samples, the permittivity of the single materials was measured at multiple points. In particular, the permittivity of the radially heterogeneous sample approximately composed of 50% Phantom A and 50% Phantom B was measured and compared to the mean relative permittivity value obtained by averaging the individual relative permittivity values of Phantom A and Phantom B, respectively. Thus, we found that the measured mean permittivity at the phantom interface is approximately equal to the calculated mean.

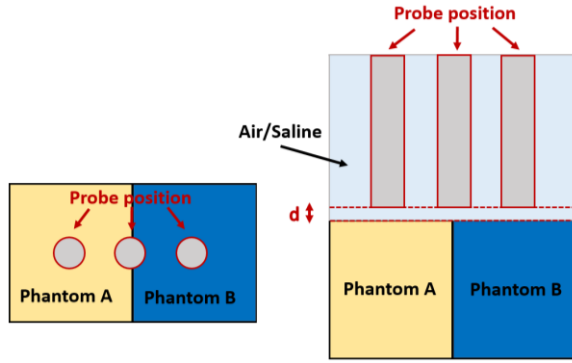


Figure 1: Diagram of the measurement set-up: on the left, top view and, on the right, front view of the combined phantoms in air or immersed in saline. In both the views, the probe position on each phantom and on the phantom interface is highlighted (with red circles in the top view and red squares in the front view). On the right, also the variable thickness of the first layer material,  $d$ , is specified.

Next, per each sample, we compared the histology depths estimated at the three measurement locations where the second layer material is: Phantom A, Phantom B, and approximately 50% Phantom A and 50% Phantom B. In consideration of the histology depth dependence on the measurement frequency, we calculated the histology depth at three frequencies: 0.5, 8.5 and 20 GHz. However, we report only the data acquired at 8.5 GHz, since the outcome is the same as for the data at the other two frequencies. In Fig. 2, the histology depths obtained at 8.5 GHz from the three measurement regions are reported for the two samples, one having saline and the other one having air as first layer material. In both plots, per each measurement location, the relative permittivity measured at different probe-material interface distances is reported. Specifically, data is plotted at probe-material interface distances: 0, 0.1, 0.2, 0.4, 0.5, 0.6, 0.7, 0.8, 0.9, 1, 1.1, 1.2, 1.3, 1.4, and 1.5 mm. In particular, we highlighted the histology depths, which are the probe-material interface distances at which the second layer material ceases to contribute to the measured dielectric properties, within the uncertainty of the measurement. Precisely, since the measurement uncertainty is 2.5 %, the histology depths from the sample composed of saline correspond to the distances at which the measured permittivity differs 2.5% from the saline permittivity (around 64 at 8.5 GHz). Alternately, the histology depths from the sample composed of air correspond to the distances at which the measured permittivity differs 2.5% from the air permittivity (around 1 across all the spectrum). From Fig. 2a, where data from the sample composed of saline is reported, we observe that the histology depth estimated on Phantom B is 0.2 mm, the one estimated on Phantom A is 0.6 mm, and the histology depth estimated at the phantom interface is 0.4 mm. In Fig. 2b, data from the sample composed of air is reported, and the estimated histology depths are 0.1, 0.3, and 0.2

for Phantom A, Phantom B, and phantom interface, respectively.

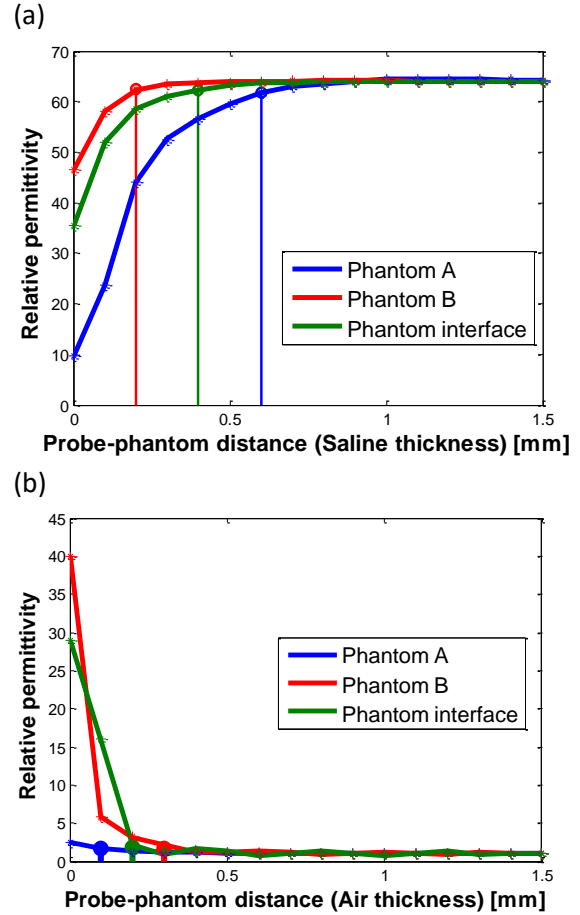


Figure 2: Estimation of the histology depths obtained from the two samples, one having saline (a) and the other one having air (b) as first layer material. Per each sample, the histology depth is estimated at three measurement locations where the second layer material is: Phantom A, Phantom B and the phantom interface. In both plots, relative permittivity data obtained at 8.5 GHz and measured at different probe-material interface distances is reported. Specifically, data is measured at probe-material interface distances ranging from 0 to 1.5 mm with 0.1 mm discrete steps.

Although the results shown in Fig. 2 form only one set of measurements (from one calibration), the same trend was found for the other two sets of recorded measurements (after the other two calibrations).

From the results obtained from both samples, it is clear that the histology depth from the radially heterogeneous phantom (made of 50% Phantom A and 50% Phantom B) is midway between the histology depths from the two constituent phantoms. This is due to the different permittivity magnitude of the second layer materials and their contrast in permittivity with the first layer material, at each measurement location. In fact, from both samples, we observe that the histology depth increases with the permittivity contrast of the layered materials. In particular, in both samples, we find that the smaller histology depths are

estimated at the measurement locations where the first and the second layer materials have low contrast in permittivity. Alternately, the larger histology depths are estimated at the measurement locations where the first and the second layer materials have high contrast in permittivity.

Also, from the comparison of the results from the two samples, we observe that the histology depth depends strongly from the permittivity magnitude of the first layer material. In particular, the histology depths from the sample composed of saline are higher than the ones from the sample composed of air. Thus, the histology depth is larger when the material in contact with the probe (first layer material) has higher permittivity, regardless of the second layer material permittivity. This finding is consistent with the histology depth analysis in [7].

In summary, we demonstrate that the histology depth is, not only dependent on the dielectric properties of the materials occupying the longitudinal extent of the histology region, but also on the dielectric properties of the materials occupying the radial extent of the histology region.

This outcome highlights the necessity of quantitatively estimating the dielectric contribution of each constituent material based on the material permittivity and spatial distribution within the interrogated region. Further experimental and numerical studies are needed in order to improve the correspondence between histological and dielectric properties of biological tissues.

#### 4 CONCLUSION

In this study, tissue-mimicking materials were used to investigate the sample histology region. In particular, after finding that the permittivity measured on a radially heterogeneous sample composed of two side by side materials is an average of the permittivities of the constituent materials, we demonstrated that also the histology depth of the radially heterogeneous sample is midway between the histology depths of the constituent materials. In addition, we verified that the histology depth increases with the permittivity magnitude of the material in contact with the probe and with the dielectric contrast of the longitudinal materials.

The experimental outcome suggests that, without careful tissue characterisation, significant errors are introduced in the interpretation of the histology region and, consequently, in the dielectric data of the investigated tissue sample. Thus, this work provides the basis for more accurate dielectric characterisation of heterogeneous tissues to support microwave medical device design.

#### Acknowledgments

The research leading to these results has received funding from the European Research Council under the ERC Grant Agreement BioElecPro n. 637780: "BIOELECTRO". This work was also supported by the Hardiman Research Scholarship. This work has been developed in the framework of COST Action MiMed (TD1301).

#### References

- [1] T. W. Athey, M. A. Stuchly, and S. S. Stuchly, "Measurement of radio frequency permittivity of biological tissues with an open-ended coaxial line: Part I," *IEEE Trans. Microw. Theory Tech.*, vol. 30, no. 1, pp. 82–86, 1982.
- [2] M. Lazebnik, L. McCartney, D. Popovic, C. B. Watkins, M. J. Lindstrom, J. Harter, S. Sewall, A. Magliocco, J. H. Booske, M. Okoniewski, and S. C. Hagness, "A large-scale study of the ultrawideband microwave dielectric properties of normal breast tissue obtained from reduction surgeries," *Phys. Med. Biol.*, vol. 52, no. 10, pp. 2637–2656, 2007.
- [3] C. Gabriel and A. Peyman, "Dielectric measurement: error analysis and assessment of uncertainty," *Phys. Med. Biol.*, vol. 51, no. 23, pp. 6033–6046, 2006.
- [4] T. Sugitani, S. Kubota, S. Kuroki, K. Sogo, K. Arihiro, M. Okada, T. Kadoya, M. Hide, M. Oda, and T. Kikkawa, "Complex permittivities of breast tumor tissues obtained from cancer surgeries," *Appl. Phys. Lett.*, vol. 104, no. 25, p. (253702)1-5, 2014.
- [5] D. M. Hagl, D. Popovic, S. C. Hagness, J. H. Booske, and M. Okoniewski, "Sensing volume of open-ended coaxial probes for dielectric characterization of breast tissue at microwave frequencies," *IEEE Trans. Microw. Theory Tech.*, vol. 51, no. 4 I, pp. 1194–1206, 2003.
- [6] P. M. Meaney, A. Gregory, N. Epstein, and K. D. Paulsen, "Microwave open-ended coaxial dielectric probe: interpretation of the sensing volume re-visited," *BMC Med. Phys.*, vol. 14, no. 1, p. 3, 2014.
- [7] P. M. Meaney, A. P. Gregory, J. Seppala, T. Lahtinen, J. Seppälä, and T. Lahtinen, "Open-Ended Coaxial Dielectric Probe Effective Penetration Depth Determination," *IEEE Trans. Microw. Theory Tech.*, vol. 64, no. 3, pp. 915–923, 2016.
- [8] E. Porter, A. La Gioia, and M. O. Halloran, "Impact of Histology Region Size on Measured Dielectric Properties of Biological Tissues," pp. 1–7.
- [9] T. Overview, "Keysight N1501A Dielectric Probe Kit 10 MHz to 50 GHz."
- [10] A. Peyman, B. Kos, M. Djokić, B. Trotošek, C. Limbaeck-Stokin, G. Serša, and D. Miklavčič, "Variation in dielectric properties due to pathological changes in human liver," *Bioelectromagnetics*, vol. 36, no. 8, pp. 603–612, 2015.
- [11] A. Peyman, C. Gabriel, and E. H. Grant, "Complex permittivity of sodium chloride solutions at microwave frequencies," *Bioelectromagnetics*, vol. 28, no. 4, pp. 264–274, 2007.
- [12] A. Santorelli, O. Laforest, E. Porter, and M. Popovi, "Image Classification for a Time-Domain Microwave Radar System: Experiments with Stable Modular Breast Phantoms," *Eur. Conf. Antennas Propag.*, 2015.